EPJ Web of Conferences **60**, 20030 (2013)
DOI: 10.1051/epjconf/20136020030

Spin and Parity Measurements of the Higgs-Like Boson in the $H \to ZZ \to 4l$ Channel at CMS

D. Austin Belknap[1,a] (CMS Collaboration)

[1] *University of Wisconsin – Madison*

Abstract. The most recent CMS results are presented for an analysis of the spin and parity of the Higgs-like boson near 126 GeV in the ZZ decay channel where the Z bosons decay into two muons or electrons. The analysis utilizes the full dataset recorded by CMS of 5.1 fb^{-1} and 19.6 fb^{-1} of pp collisions at center-of-mass energies of $\sqrt{s}$ = 7 and 8 TeV respectively. The Standard Model prediction is compared against six alternate J^P hypotheses. In all cases, the data favor the Standard Model prediction.

1 Introduction

On 4 July 2012, the CMS and ATLAS collaborations announced the discovery of a new boson with a mass near 125 GeV that was consistent with the Higgs boson. Characterization of the properties of this new boson is essential to determine whether or not this new particle is a Higgs boson as predicted in the Standard Model. Presented here are results from the CMS experiment pertaining to spin and parity measurements of this new particle in the $H \to ZZ \to 4l$ channel.

2 Event Selection

In the $H \to ZZ \to 4l$ channel, we consider the following final states: $4e$, 4μ, and $2e2\mu$. We require that events pass either the Double Muon, Double Electron, Triple Electron, or Muon + Electron triggers. The fiducial cuts placed on the leptons are $p_T > 5$ GeV and $|\eta| < 2.4$ for muons, and $p_T > 7$ GeV and $|\eta| < 2.5$ for electrons.

To select the Z candidates, leptons are combined into opposite-sign same-flavor pairs. The pair closest to the nominal Z mass is selected as Z_1. The remaining pair with the highest p_T scalar sum is selected as Z_2.

We also include Final State Radiation (FSR) photons. Photons are first assigned to their nearest lepton. If the leptons of a Z candidate have FSR candidates, an FSR photon is selected if it brings the Z candidates mass closer to nominal. At most, one photon may be assigned to a Z candidate.

The leptons are required to have a relative isolation < 0.4 with an isolation cone of $\Delta R < 0.4$. If a lepton's FSR photon was selected, that photon is not included in the lepton's isolation sum.

The following phase-space cuts are placed on the Z masses: $40 < m_{Z1} < 120$ GeV and $12 < m_{Z2} < 120$ GeV.

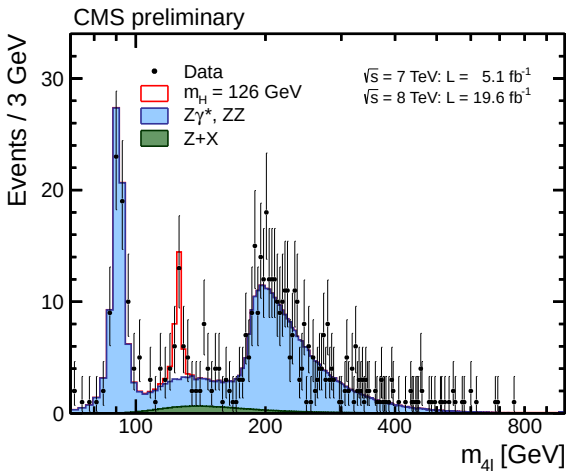

Figure 1. Shown here is the 4-lepton invariant mass distribution for the $4e$, 4μ, and $2e2\mu$ final states. The data are shown as solid points, which are compared to the total expected distributions of signal and all backgrounds. The unshaded histogram represents the expected signal, and the shaded histograms represent the backgrounds. The signal strength of the new boson with respect to the Standard Model expectation is $\mu = 0.91^{+0.30}_{-0.24}$.

To accommodate the trigger thresholds, at least one lepton should satisfy $p_T > 20$ GeV and another $p_T > 10$ GeV.

The spin-parity analysis considers events in the signal region where $106 < m_{4l} < 141$ GeV as seen in Figure 1.

3 Spin and Parity Measurements

Determining the spin and parity of the Higgs-like particle is done by testing the Standard Model hypothesis ($J^P = 0^+$) against alternate spin-parity hypotheses. The six alternate hypotheses considered are

[a] e-mail: dabelknap@wisc.edu

Table 1. The spin-parity hypotheses tested are listed in the table below. The expected significance is given with the signal strength calculated from data, and when $\mu = 1$ is assumed. The observed separations show the consistency of the data with the SM 0^+ model, or the alternate J^P models where the signal strength is calculated from the data.

J^P	Production	Comment	Expect ($\mu = 1$)	Obs. 0^+	Obs. J^P	CL_s
0^-	$gg \to X$	pseudoscalar	2.6σ (2.8σ)	0.5σ	3.3σ	0.16%
0_h^+	$gg \to X$	higher dim. operators	1.7σ (1.8σ)	0.0σ	1.7σ	8.1%
2^+_{mgg}	$gg \to X$	minimal couplings	1.8σ (1.9σ)	0.8σ	2.7σ	1.5%
$2^+_{mq\bar{q}}$	$q\bar{q} \to X$	minimal couplings	1.7σ (1.9σ)	1.8σ	4.0σ	< 0.1%
1^-	$q\bar{q} \to X$	exotic vector	2.8σ (3.1σ)	1.4σ	$> 4.0\sigma$	< 0.1%
1^+	$q\bar{q} \to X$	exotic pseudovector	2.3σ (2.6σ)	1.7σ	$> 4.0\sigma$	< 0.1%

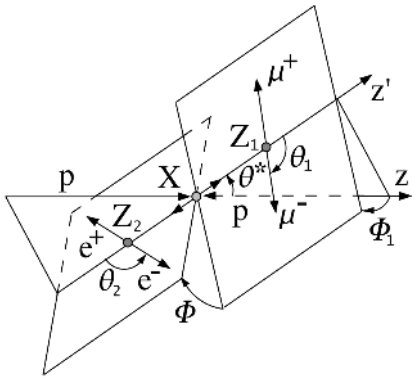

Figure 2. The production angles Φ_1 and θ^* are calculated in the rest frame of X. The decay angles θ_1 and θ_2 are shown in their respective Z rest frames. Φ is given in the X rest frame.

$J^P = 0^-$, 0_h^+, 2^+_{mgg}, $2^+_{mq\bar{q}}$, 1^+, and 1^-. We use a log-likelihood ratio test statistic that utilizes the full kinematic information of the event. The kinematics of a $H \to 4l$ event can be described fully with the five angles θ^*, Φ_1, θ_1, θ_2, and Φ (Figure 2) with the masses m_{Z1} and m_{Z2}.

- θ^* Angle between Z_1's trajectory and the beam axis
- Φ_1 Angle between the Z_1 decay plane and the X decay plane
- $\theta_{1,2}$ Angle between the negative lepton trajectory and the trajectory of its parent Z
- Φ Angle between the decay planes of the two Zs

In order to more strongly distinguish between the spin-parity hypotheses, we wish to discriminate against the backgrounds. Using a matrix element likelihood approach [2], a discriminant is constructed in order to distinguish the possible signal hypotheses from the backgrounds

$$\mathcal{D}_{bkg} = \frac{\mathcal{P}_{sig}}{\mathcal{P}_{sig} + \mathcal{P}_{bkg}}. \quad (1)$$

This discriminant utilizes all decay angles, m_{Z1}, m_{Z2}, as well as the m_{4l} distribution for $m_H = 126$ GeV.

The shapes of this discriminant for the different signal hypotheses are very similar, but differ considerably from the backgrounds.

To distinguish between the Standard Model and an alternative J^P hypothesis, a discriminant is calculated utilizing a matrix element likelihood approach with the observables m_{Z1}, m_{Z2}, and the decay angles $\vec{\Omega}$.

$$\mathcal{D}_{J^P} = \frac{\mathcal{P}_{SM}}{\mathcal{P}_{SM} + \mathcal{P}_{J^P}} = \left[1 + \frac{\mathcal{P}_{J^P}\left(m_{Z1}, m_{Z2}, \vec{\Omega}|m_{4l}\right)}{\mathcal{P}_{SM}\left(m_{Z1}, m_{Z2}, \vec{\Omega}|m_{4l}\right)}\right]^{-1} \quad (2)$$

Distributions of the value of $\mathcal{D}_{J^P}$ seen in Figure 3 show the discrimination between the 0^+ and alternate hypotheses.

We then build a 2D log-likelihood ratio test statistic from the discriminants ($\mathcal{D}_{bkg}, \mathcal{D}_{J^P}$):

$$q = -2\ln\left[\frac{\mathcal{L}_{J^P}}{\mathcal{L}_{SM}}\right]. \quad (3)$$

The values for the test statistic q (Equation 3) are shown as distributions for the 0^+ and alternate J^P cases, and the value observed from data is indicated by an arrow in Figure 4. From these distributions, we can see the level of separation the $\mathcal{D}_{J^P}$ discriminant provides. The expected and observed significance for each of the tests are given in Table 1. It is seen that when compared with the six alternate J^P hypotheses, the Standard Model pure scalar hypothesis is favored by the data.

References

[1] CMS Collaboration, CMS-PAS-HIG-13-002

[2] S. Chatrchyan et al. (CMS Collaboration), Phys.Lett. **B716**, 30 (2012), 1207.7235

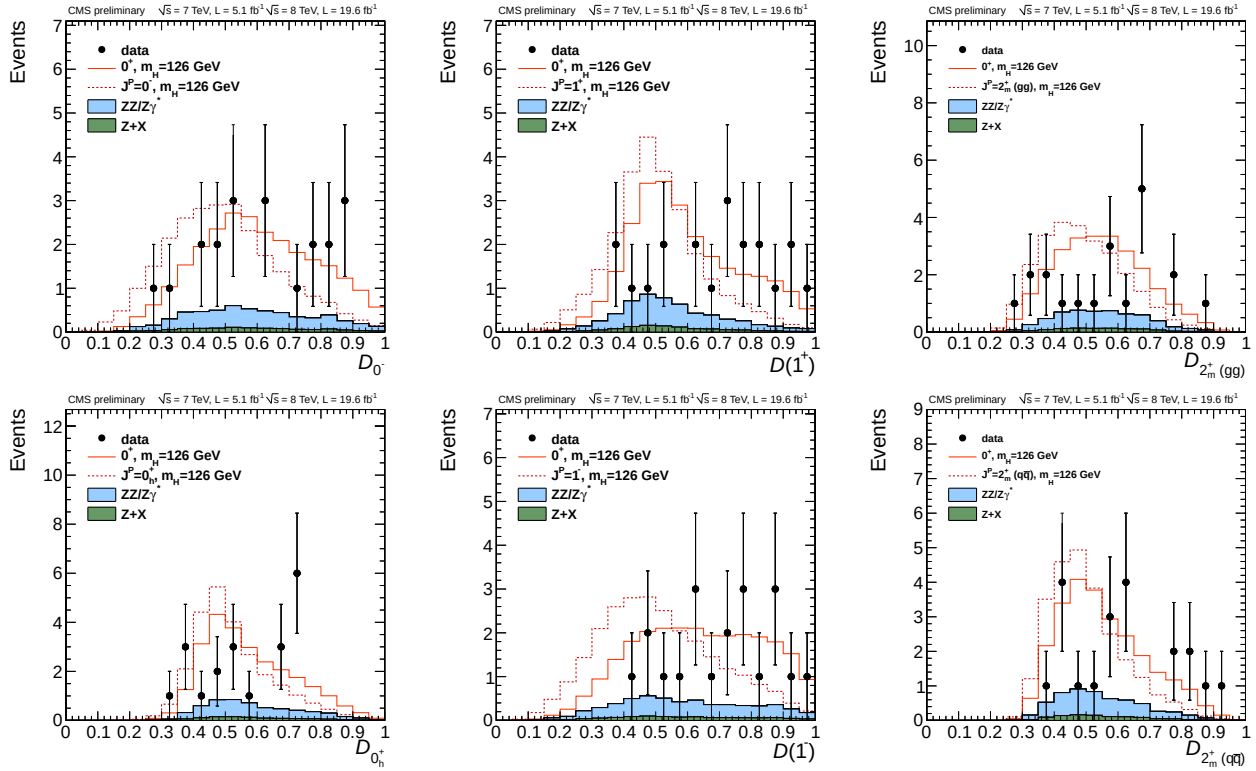

Figure 3. The distributions of the discriminant $\mathcal{D}_{J^P}$ are shown with the requirement $\mathcal{D}_{bkg} > 0.5$. The expected signal and background distributions are shown with the data shown as points with error bars. From top to bottom, left to right, the hypotheses tested are $J^P = 0^-,\ 0_h^+,\ 1^+,\ 1^-,\ 2_m^+(gg)$, and $2_m^+(q\bar{q})$.

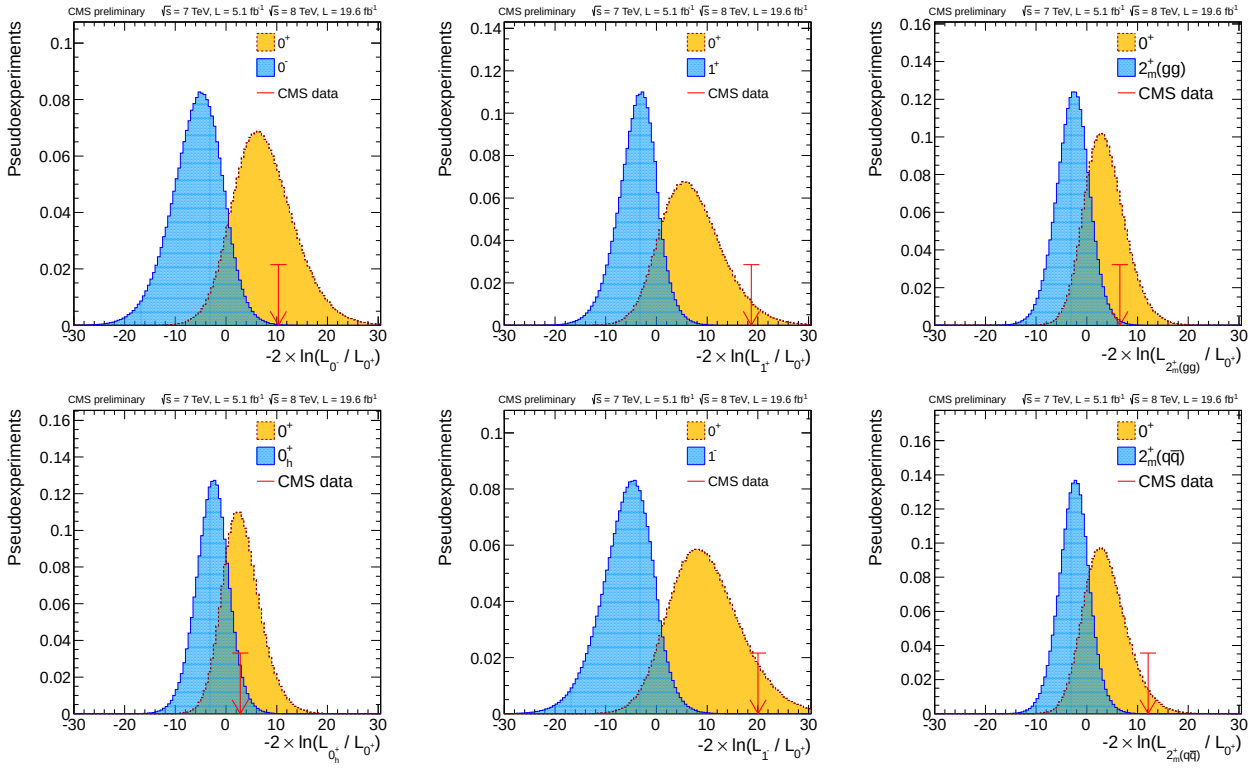

Figure 4. The test statistic $q = -2\ln(\mathcal{L}_{J^P}/\mathcal{L}_{SM})$ is shown for the SM 0^+ model (blue) and the alternate J^P hypothesis (yellow). The expected distributions are generated by generating Monte Carlo experiments assuming $m_H = 126$ GeV. The value observed from the data is indicated by a red arrow. From top to bottom, left to right, the hypotheses tested are $J^P = 0^-,\ 0_h^+,\ 1^+,\ 1^-,\ 2_m^+(gg)$, and $2_m^+(q\bar{q})$.